On the Use of Radar Depolarization Ratios for Estimating Shapes of Ice Hydrometeors in Winter Clouds

SERGEY Y. MATROSOV

*Cooperative Institute for Research in the Environmental Sciences, University of Colorado, and
NOAA/Environmental Technology Laboratory, Boulder, Colorado*

ROGER F. REINKING, ROBERT A. KROPFLI, BROOKS E. MARTNER, AND B. W. BARTRAM

NOAA/Environmental Technology Laboratory, Boulder, Colorado

ABSTRACT

An approach is suggested to relate measurements of radar depolarization ratios and aspect ratios of predominant hydrometeors in nonprecipitating and weakly precipitating layers of winter clouds. The trends of elevation angle dependencies of depolarization ratios are first used to distinguish between columnar-type and plate-type particles. For the established particle type, values of depolarization ratios observed at certain elevation angles, for which the influence of particle orientation is minimal, are then used to estimate aspect ratios when information on particle effective bulk density is assumed or inferred from other measurements. The use of different polarizations, including circular, slant-45° linear, and two elliptical polarizations, is discussed. These two elliptical polarizations are quasi-circular and quasi-linear slant-45° linear, and both are currently achievable with the National Oceanic and Atmospheric Administration Environmental Technology Laboratory's K_a-band radar. In comparison with the true circular and slant-45° linear polarizations, the discussed elliptical polarizations provide a stronger signal in the ''weak'' radar receiver channel; however, it is at the expense of diminished dynamic range of depolarization ratio variations. For depolarization measurements at the radar elevation angles that do not show much sensitivity to particle orientations, the available quasi-circular polarization provides a better depolarization contrast between nonspherical and spherical particles than does the available quasi-linear slant-45°polarization. The use of the proposed approach is illustrated with the experimental data collected during a recent field experiment. It is shown that it allows successful differentiation among pristine planar crystals, rimed planar crystals, long columns, blocky columns, and graupel. When a reasonable assumption about particle bulk density is made, quantitative estimates of particle aspect ratios from radar depolarization data are in good agreement with in situ observations. Uncertainties of particle aspect ratios estimated from depolarization measurements due to 0.1 g cm^{-3} variations in the assumed bulk density are about 0.1.

1. Introduction

Millimeter-wavelength polarization radar is a powerful tool for studying clouds. It offers a unique means to distinguish among different types of cloud particles. One radar polarization parameter that can be used for this purpose is the depolarization ratio because various cloud particles depolarize the incident electromagnetic wave differently according to their phase (i.e., ice vs water), general shape (e.g., oblate vs prolate), aspect ratio, orientation, and bulk density. Several studies using some specific transmit polarization states demonstrated the utility of the depolarization ratio approach for identifying cloud particles (e.g., Matrosov et al. 1996; Re-

inking et al. 1997a, 1997b). The outcome of this research can have direct applications to cloud physics, climate research, and aircraft icing avoidance.

Since 1993, the National Oceanic and Atmospheric Administration's (NOAA) Environmental Technology Laboratory (ETL) has been pursuing studies of winter clouds with its ''NOAA/K'' K_a-band radar ($\lambda = 8.66$ mm) under different phases of the Winter Icing and Storms Program (WISP). This transportable Doppler radar has an offset Cassegrain antenna; a rotatable phase retarding plate (PRP) is used to change polarization of transmitted signals (Matrosov and Kropfli 1993). Two receivers measure backscattered power simultaneously in two orthogonal polarizations, thus allowing measurements of depolarization ratio.

Progress has been made for identifying different species of hydrometeors in precipitating cloud systems (i.e., rain of different intensity, hail, snow, cloud ice, etc.) with the use of S-band polarization radars (e.g., Vivek-

Corresponding author address: Dr. Sergey Y. Matrosov, R/E/ET6, 325 Broadway, Boulder, CO 80303.
E-mail: smatrosov@etl.noaa.gov

anandan et al. 1999; Zrnić and Ryzhkov 1999). However, the use of the K_a-band wavelength, which is inherently more sensitive to small particles than are standard meteorological radar wavelengths ($\lambda \sim 5$–11 cm), makes this radar suitable for observations of nonprecipitating and weakly precipitating winter clouds and for identifying different species of cloud ice particles. Additional advantages of K_a-band radars include a very good spatial resolution (typically 37.5 m with the ETL K_a-band radar) and reduced ground clutter (Kropfli and Kelly 1996), which allows these radars to collect useful data starting at close ranges as short as a few hundred meters while allowing observations to be made at ranges of several tens of kilometers.

Most polarization diversity radars used in meteorology utilize either horizontally or circularly polarized signals. The quasi-optical technology of the PRP hardware utilized by the ETL K_a-band radar allows the use of different states of elliptical polarizations. Circular polarization and different orientations of linear polarization can be obtained with quarter-wave and half-wave PRPs that have phase shifts of exactly 90° and 180°, respectively. Manufacturing a PRP with the exact desired phase shift at K_a-band frequencies is very difficult. Calibrations revealed that the first PRP used in earlier WISP experiments had a phase shift of about 79° rather than 90°, for example. However, the use of the elliptical polarization obtained with that PRP proved to be beneficial for studies of low reflectivity clouds, since it provided a significant increase of the received power in the ''weak'' polarization channel.

Two new PRPs were recently manufactured for use with the ETL K_a-band radar. The calibrations of these PRPs in drizzle indicated their phase shifts to be about 88° (quasi–quarter-wave plate) and 177.4° (quasi–half-wave plate), which are relatively close to the target values (i.e., 90° and 180°, respectively). In spite of this, depolarization ratios with the resulting actual polarization states could differ significantly (depending on the PRP rotation) from the depolarization ratios with perfect circular and linear polarizations.

The main objective of this paper is to investigate the use of true circular and linear polarizations as well as quasi-circular and quasi-linear polarizations available with the ETL K_a-band radar for inferring shape parameters of cloud particles. We limit the discussion here by considering only depolarization ratios, although other

radar polarization parameters can also be potentially used for this purpose. The main reason behind this consideration is that depolarization measurements are the already proven tool for such tasks, and it is currently the polarization parameter routinely measurable with the ETL K_a-band radar.

2. Theoretical considerations

The simplest geometric shape that enables the modeling of radar polarization properties of hydrometeors is that of a spheroid. Since our radar wavelength is significantly greater than the particle dimensions, the scattering properties depend largely on the overall shape and not on subtle differences in particle structure (Dungey and Bohren 1993), which justifies the assumption of this relatively simple shape. Plate-type crystals, including stellars and dendrites, are usually modeled as oblate spheroids, and the columnar-type crystals (i.e., columns, bullets, and needles) are modeled as prolate spheroids with the corresponding aspect ratios, r (i.e, the minor-to-major axis length ratio). Aggregation results in an effective increase of r and decrease of particle bulk density, but the spheroidal shape is still adequate to describe aggregate polarization properties (Matrosov et al. 1996).

Aside from snowfalls, typical sizes of particles in winter clouds usually do not exceed about 2 mm, and the Rayleigh theory (see, e.g., Bohren and Huffman 1983) is still applicable for calculations of radar reflectivities at K_a-band wavelengths with an accuracy of 1 dB or so, which is comparable to the uncertainty of the radar absolute calibration. In this study, we are mostly concerned with depolarization ratios for which the Rayleigh approximation accuracy is acceptable.

a. Amplitude backscattering matrix

The backscatter characteristics of a single spheroidal particle can be described in terms of the scattering amplitudes for the horizontal (s_{hh}) and vertical (s_{vv}) polarizations in the linear basis. In the optical convention, the scattering matrix $\mathbf{S}$, which defines transformations of the amplitude vector of the incident signal, can be given as (Bohren and Huffman 1983; Matrosov and Kropfli 1993)

$$\mathbf{S} = \frac{e^{ikl}}{-ikl}\begin{bmatrix} s_{hh}\cos^2\alpha - s_{vv}\sin^2\alpha & -(s_{hh} + s_{vv})\sin\alpha\,\cos\alpha \\ (s_{hh} + s_{vv})\sin\alpha\,\cos\alpha & s_{vv}\cos^2\alpha - s_{hh}\sin^2\alpha \end{bmatrix}, \tag{1}$$

where k and l are the wavenumber and the distance from the scatterer, respectively. Here, α is the particle canting

angle, which is related to the angles θ and ϕ describing the orientation of particle symmetry axis in the spherical

coordinate system; the radar elevation angle χ; and angle ψ between the incident electromagnetic wave propagation vector and the particle symmetry axis (Holt 1984):

$$\cos\alpha \ \sin\psi = \cos\theta \ \cos\chi + \sin\theta \ \sin\chi \ \cos\phi,$$

$$\sin\alpha \ \sin\psi = \sin\theta \ \sin\phi,$$

$$\cos\psi = \cos\theta \ \sin\chi - \sin\theta \ \cos\phi \ \cos\chi. \quad (2)$$

The matrix (1) describes the transformation of the amplitude vector of the incident electromagnetic wave due to backscattering. The amplitude s_{hh} is equal to the principal scattering amplitude along the axis that is perpendicular to the particle symmetry axis (s_2). The amplitude s_{vv} can be expressed in terms of s_2 and the principal scattering amplitude along the particle symmetry axis (s_1):

$$s_{hh} = s_2 \qquad s_{vv} = s_1 \sin^2\psi - s_2 \cos^2\psi. \quad (3)$$

Note that s_{hh} and s_{vv} have opposite signs in the convention adopted here.

The polarization state incident on the PRP is horizontal, and the corresponding amplitude vector for a perfect antenna is given by the unit vector

$$\mathbf{E}_h = \begin{pmatrix} 1 \\ 0 \end{pmatrix}. \quad (4)$$

This incident polarization is changed by the PRP. In the event when the PRP axes are parallel to the linear polarization basis unit vectors, this change is given by the matrix $\mathbf{R}(\Psi)$ in terms of the PRP phase shift angle Ψ (Shurcliff 1962):

$$\mathbf{R}(\Psi) = \begin{bmatrix} e^{i\Psi} & 0 \\ 0 & 1 \end{bmatrix}. \quad (5)$$

In a general case, when the PRP slow axis is rotated at an angle β with respect to $\mathbf{E}_h$, additional rotation matrices $\mathbf{T}(\beta)$ should be used to describe the corresponding polarization transformation

$$\mathbf{T}(\beta) = \begin{bmatrix} \cos\beta & \sin\beta \\ -\sin\beta & \cos\beta \end{bmatrix}. \quad (6)$$

The combined effects of backscattering and the transformations by the PRP on the transmitted and received signals are given by the matrix product $\mathbf{T}(\beta)\mathbf{R}(\Psi)\mathbf{T}(-\beta)\mathbf{S}\mathbf{T}(-\beta)\mathbf{R}(\Psi)\mathbf{T}(\beta)$.

Round-trip propagation effects along the propagation path l_o can also be accounted for by means of the propagation matrix $\mathbf{U}$. If α_0, the mean canting angle of particles along the path, is zero, then this matrix is diagonal (Oguchi 1983):

$$\mathbf{U} = \begin{bmatrix} \exp(-2\pi l_o f_{hh}/k^2) & 0 \\ 0 & \exp(-2\pi l_o f_{vv}/k^2) \end{bmatrix}, \quad (7)$$

where the quantities f_{ii} ($i = h$ or v) are determined by the integration over the particle size distribution $N(D)$ along the propagation path

$$f_{ii} = \int_0^{D_{\max}} N(D)s_i[\exp(-2\sigma_1^2) \cos(2\gamma) + 1] \exp(-2\sigma_2^2) \, dD. \quad (8)$$

In (8), γ is the mean angle between the particle symmetry axes and their projections on the propagating wave polarization plane, and σ_1 and σ_2 are the standard deviations of γ and the canting angle α_0, respectively. Note that amplitudes s_h and s_v are the same as s_2 and s_1 in (3) (except for the opposite sign for s_v), since we consider the Rayleigh scattering regime.

If α_0 is not zero, the rotation matrices $\mathbf{T}$ should be applied before and after applying the propagation matrix $\mathbf{U}$. Assuming that hydrometeors have the same properties along the whole propagation path, the electrical vector of the backscattered electromagnetic wave $\mathbf{E}_b$ can be calculated using the following matrix multiplication:

$$\mathbf{E}_b = C_R\mathbf{T}(\beta)\mathbf{R}(\Psi)\mathbf{T}(-\beta)\mathbf{T}(\alpha_0)\mathbf{U}\mathbf{T}(-\alpha_0)\mathbf{S}\mathbf{T}(-\alpha_0)$$

$$\times \ \mathbf{U}\mathbf{T}(\alpha_0)\mathbf{T}(-\beta)\mathbf{R}(\Psi)\mathbf{T}(\beta)\mathbf{E}_h = C_R\mathbf{Y}\mathbf{E}_h, \quad (9)$$

where C_R is the constant that depends on the radar characteristics and the range to the scatterer, and $\mathbf{Y}$ is the resulting matrix.

b. Depolarization ratios

The ETL K_a-band radar measures backscattered signal powers in the copolar (P_{co}) and cross polar (P_{cr}) receivers. These powers can be calculated from elements of matrix $\mathbf{Y}$ accounting for the scatterer distributions

$$P_{co} = \langle y_{11}y_{11}^* \rangle C, \qquad P_{cr} = \langle y_{12}y_{12}^* \rangle C, \quad (10)$$

where C is a constant, * means complex conjugation, and the angular brackets represent averaging with respect to particle sizes, shapes, and orientations within the radar resolution volume.

The logarithmic difference between P_{cr} and P_{co} is defined as the depolarization ratio (DR). The relative magnitude of P_{cr} and P_{co} changes with the incident polarization (i.e., with the PRP phase shift angle Ψ). For the linear polarization $P_{cr} < P_{co}$, and for the circular polarization $P_{cr} > P_{co}$. Since it is customary to express depolarization ratios as negative values and we consider
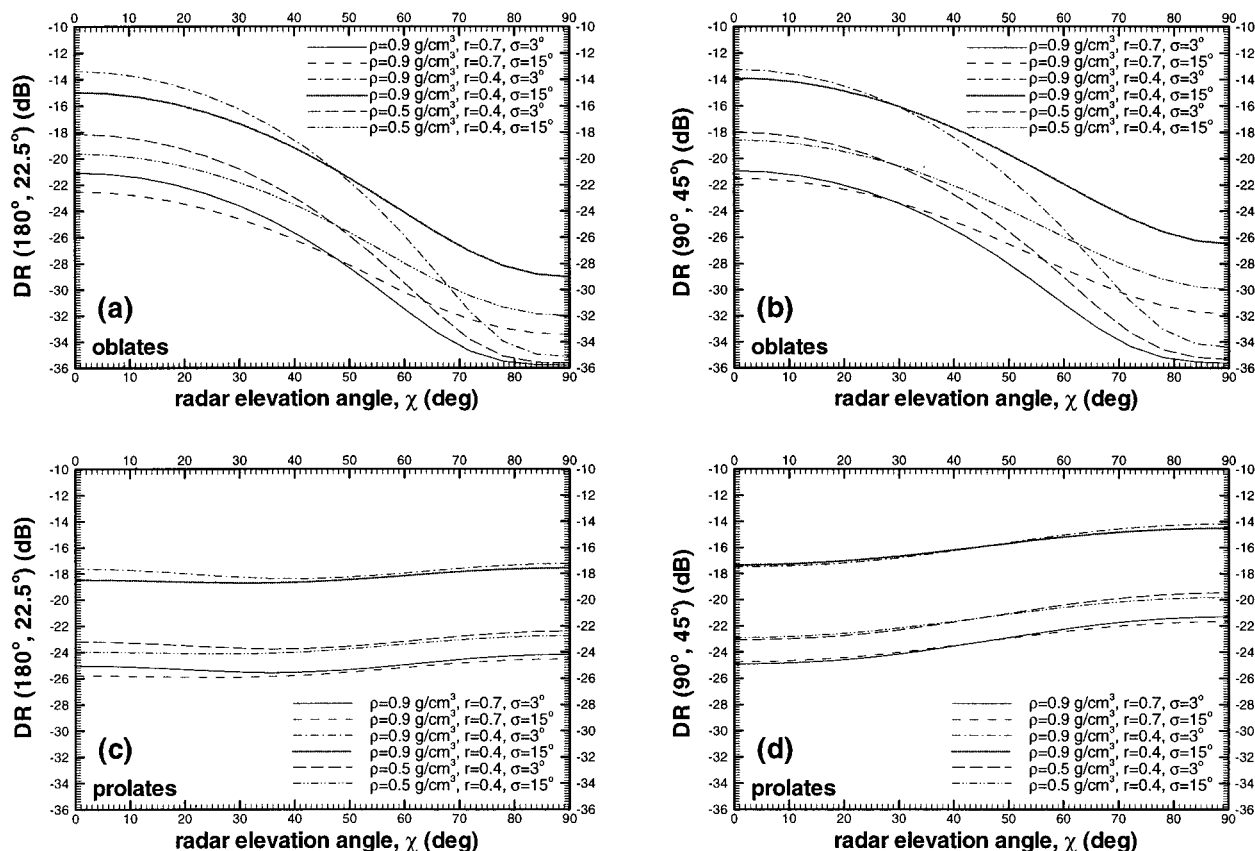
FIG. 1. Slant-45° linear (a and c) and circular (b and d) depolarization ratios as a function of the radar elevation angle for different oblate (a and b) and prolate (c and d) particle aspect ratios r and densities ρ.

here polarizations in the vicinity of both linear and circular polarizations, we define

$$\mathrm{DR} = 10 \log_{10}[\min(P_{cr}, P_{co})/\max(P_{cr}, P_{co})]. \quad (11)$$

The polarization of transmitted radar signals is determined by two angles: Ψ and β. To specify this fact, we will use a generic definition of DR and indicate these angles as arguments [i.e., $\mathrm{DR}(\Psi, \beta)$]. Note that the conventional linear (LDR) and circular (CDR) depolarization ratios can be expressed as $\mathrm{DR}(\xi, 0°)$ and $\mathrm{DR}(90°, 45°)$, respectively (where ξ is any phase shift angle).

3. Results of DR modeling

In the absence of strong electrical fields, aerodynamic forcing tends to orient ice particles randomly with their major dimensions in the horizontal plane (Sassen 1980). We will assume such orientation for our modeling, allowing, however, some flutter, which is described by the standard deviation from the preferable horizontal orientation, σ.

Because ice particles often have the effective bulk density ρ less than that for solid ice ($\rho_i = 0.9 \mathrm{~g~cm^{-3}}$), the complex refractive index m, which is needed to compute the scattering amplitudes along the spheroidal prin-

cipal axis (i.e., s_h and s_v), was calculated using Wiener's rule for ice–air mixtures:

$$\rho_i \frac{m^2 - 1}{m^2 + 2} \approx \rho \frac{m_i^2 - 1}{m_i^2 + 2}. \quad (12)$$

For K_a-band frequencies at a temperature $-10°C$, $m_i = (1.78, 0.004)$. The principal axes scattering amplitudes were calculated using the well-known Rayleigh regime equations (see, e.g., Bohren and Huffman 1983).

As was shown in Matrosov (1991), depolarization ratios in the traditional horizontal–vertical (H–V) linear basis (i.e., LDR) strongly depend on the canting angle, and LDR values are very small (i.e., the radar echo in the "weak" channel is small) at low elevation observations when this angle is small. This makes the use of this polarization basis not very suitable for the purpose of identifying particle types and for estimating their aspect ratios. Rotating the linear polarization basis can alleviate this situation. It is obvious that for the preferred horizontal orientation of scatterers, depolarization ratios in the linear bases reach maximum values for the polarization basis rotated at 45° with respect to horizontal. This limitation on LDR is somewhat eased, however, for close-range aircraft-based observations when both echoes are well above the noise level. Measurements in

the H–V basis can be used then to reconstruct depolarization response for bases where the canting angle dependencies are minimal.

We performed calculations of DR for the slant-45° linear basis and circular polarizations [i.e., DR(180°, 22.5°) and DR(90°, 45°)], as well as for the elliptical polarizations achieved with the most recently manufactured PRPs [i.e., DR(177.4°, 22.5°) and DR(88°, 45°)]. An important difference from the earlier CDR calculations by Matrosov (1991) is that here, an appropriate value for the two-way polarization cross-talk of the ETL K_a-band radar antenna is accounted for (36 dB), and a wide range of different particle aspect ratios r and densities ρ was modeled instead of focusing on a few particular single crystal habits. The model calculations were performed initially ignoring the propagation effects. The influence of these effects is discussed later.

a. Elevation angle dependencies of DR

As suggested by Matrosov (1991), Matrosov et al. (1996), and Aydin and Tang (1997), elevation angle dependencies of DR can be effectively used to distinguish between layers of prolate and oblate types of hydrometeors. These dependencies for the oblate (plate-type) particles have a monotonic tendency to decrease as the radar elevation angle changes from low elevations to the zenith direction. Figures 1a and 1b show these dependencies for the slant-45° linear and circular polarizations for several particle aspect ratios $r,$ bulk densities $\rho,$ and standard deviations from the horizontal orientations, σ. Note that if r and σ are the same for all the particles, DR values do not depend on the particle size distribution function $N(D)$.

Comparisons of Figs. 1a and 1b show the similarity of DR behavior for these two polarizations. Note that for the 0° elevation and the strictly horizontal orientation of scatterers, the scattering matrices for these polarization bases are identical (Torlashi and Holt 1999). In close approximation, this result is clearly seen from comparisons of DR values at $\chi = 0°$ and $\sigma = 3°$ (almost horizontal orientation of scatterers). The dynamic range of DR variations with the elevation angle is increasing as σ is decreasing. However, DR values at $\chi \approx 48°$ for the slant-45° linear and at $\chi \approx 30°$ for the circular polarizations do not exhibit much dependence on σ and depend only on particle aspect ratio and bulk density. This fact suggests a means to separate the effects of the shape/density and orientation and to use DR measurements for quantitative estimations of particle properties. We will denote the elevation angle where the effects of particle orientation on DR values are minimal as χ_o.

Figures 1c and 1d show the DR elevation angle dependencies for prolate (columnar-type) particles for the slant-45° linear and circular polarizations. These dependencies are quite different from those for oblate particles, providing a convenient way of discriminating particle types (i.e., prolate vs oblate). There is a monotonic increase of circular polarization DR values for prolates when the elevation angle increases. The use of the slant-45° linear polarization basis results in practically constant values of DR.

The variability of DRs due to σ for prolates is very small for the whole range of radar elevations. This variability is the smallest, however, for $\chi_o \approx 45°$, which suggests that measurements at this angle can be used for quantitative estimates of particle shapes (assuming a certain value for the bulk density). The choice of such an angle for prolates is not as sensitive as for oblates, however, especially for the slant-45° linear polarization because of very small variations of DR with the radar elevation angle for this polarization. This fact makes the slant-45° linear polarization preferable to the circular polarization for the purpose of particle type identifications. An additional advantage of the slant-45° linear polarization is the fact that the independence of DRs for oblates is observed for higher elevation angles (48° for slant-45° linear vs 30° for circular), which is more convenient for making measurements of cloud layers with a limited horizontal extent. However, as it will be shown, this advantage is achieved at the expense of lower depolarization contrasts between nonspherical and spherical particles.

As mentioned earlier, the current phase retarding plates manufactured for use with the ETL K_a-band radar have phase shift angles of about 177.4° and 88°, respectively. Rotations of these plates at 22.5° and 45° with respect to horizontal orientation produce quasi-linear slant-45° and quasi-circular elliptical polarizations, with an ellipticity of about 0.03 and 0.96, correspondingly. The advantages of using elliptical polarizations that are close to circular or linear are mostly in raising power in the ''weak'' receiver channel. This allows polarization detection of lower reflectivity clouds for which ''weak'' channel signals can be below the receiver noise level if traditional (e.g., H–V basis) polarization basis is used. The improved polarization sensitivity in elliptical polarization bases is achieved, however, at the expense of lower dynamic ranges of DR changes. Higher dynamic ranges result in a better separability between different particle species. The choice of the polarization state should be dictated by a compromise between sensitivity and dynamic range issues.

Figure 2 shows elevation angle dependencies for quasi-linear slant-45° and quasi-circular polarizations achievable currently with the ETL K_a-band radar. A comparison of Figs. 1 (a and b) and 2 (a and b) for oblates reveals that the considered elliptical polarizations produce larger values of DR near the zenith direction when compared with the true slant-45° linear and circular polarizations. For low elevations, DR values are quite comparable for the elliptical and ''perfect'' polarizations. As a result, the dynamic range of DR changes with elevation is less for the elliptical polarizations.

For prolate particles (Figs. 1b, 1d, 2b, and 2d), DR values for the elliptical polarizations are slightly greater than the ones for the true slant-45° linear and circular
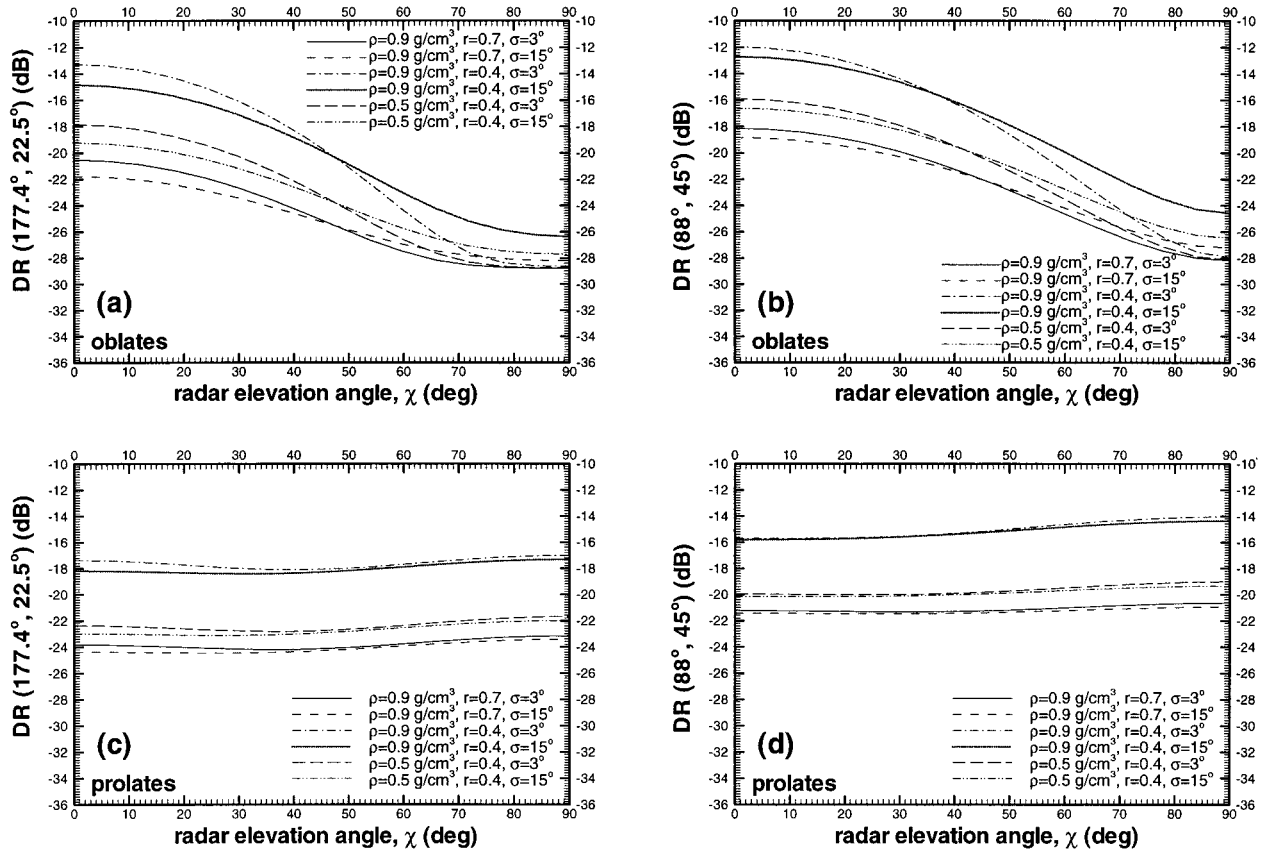
FIG. 2. Elliptical DRs for the PRP phase angles (a and c) 177.4° and (b and d) 88° as a function of the radar elevation angle for different oblate (a and b) and prolate (c and d) particle aspect ratios r and densities ρ.

polarizations at all elevation angles. Also, the elevation angle variability of prolate particle DR is less for the quasi-circular polarization (Fig. 2d) when compared with the true circular polarization (Fig. 1d).

As in the case of the true slant-45° linear and circular polarizations, the radar elevation angle $\chi_o \approx 45°$ can be considered as the one where the effects of prolate particle orientations (i.e., those of σ) are minimal. For oblates and the quasi-linear slant-45° polarization, such an angle is still about 48°, as in the case of the true slant-45° linear polarization. However, quasi-circular polarization results in some shift of this angle to higher elevations when compared with the perfect polarization case for oblates. For this polarization, χ_o varies approximately between 40° and 50° (see Fig. 2b). The DR variability due to particle orientations in this range of χ_o is relatively small, and $\chi_o \approx 45°$ can be considered to be a reasonable choice for the elevation where depolarization measurements are least affected by particle fluttering.

b. Estimation of particle aspect ratios from depolarization measurements

As indicated in the previous section, measurements of DRs at certain radar elevations χ_o are minimally af-

fected by particle flutter relative to their preferred horizontal orientation. Values of DR measured at these elevations can be used to estimate particle aspect ratios, r, if particle bulk density is known or assumed. It is more convenient to make such estimations using deviations ΔDR of DR for nonspherical particles from DR corresponding to spheres, DR_{sph}:

$$\Delta DR(\chi_o, \Psi, \beta) = DR(\chi_o) - DR_{sph}. \qquad (13)$$

For the ETL K_a-band radar, DR_{sph} values are -36 dB for the true slant-45° linear and circular polarizations and about -29 dB for both slightly elliptical polarizations considered here. The arguments of ΔDR indicate the polarization type (defined by the two angles Ψ and β) and the choice of radar elevation angle χ_o. According to this definition, the parameter ΔDR is greater than 0 for nonspherical particles randomly oriented in the horizontal plane.

For the perfect slant-45° linear and circular polarizations, Fig. 3 depicts ΔDR as a function of particle aspect ratios. Symbols in this figure indicate results of model calculations for different bulk densities. The results are rather similar for both perfect polarizations; however, the circular polarization ΔDR values are slightly larger, thus providing a better contrast. The dif-
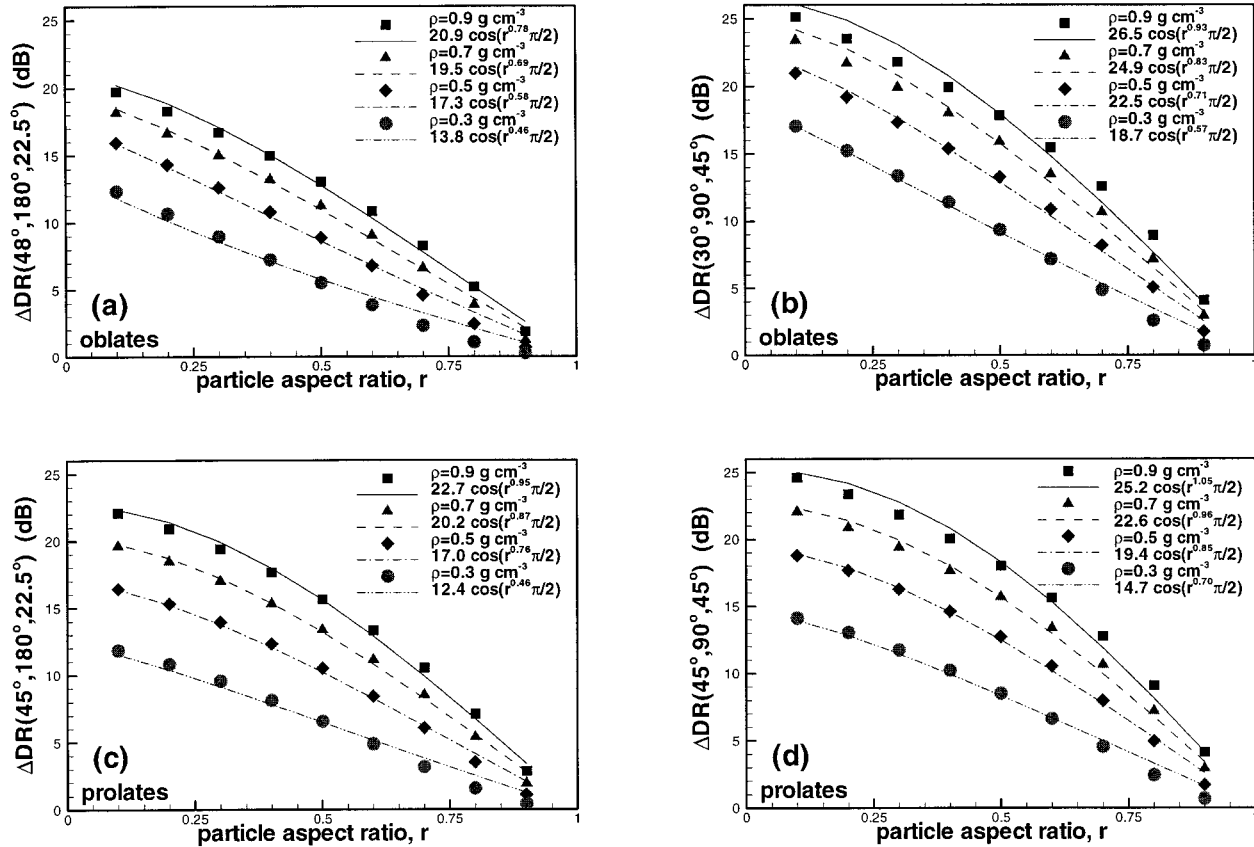
FIG. 3. Depolarization difference as a function of (a and b) oblate and (c and d) prolate particle aspect ratios for the slant-45° linear (a and c) and circular (b and d) polarizations.

ferentiation from the spherical shape becomes less pronounced as the particle bulk density decreases.

The calculated results were approximated in terms of particle aspect ratios r by analytical functions represented by cosines. Cosines provided a much better fit than power-law or exponential fits. The approximations are shown by curves, and their coefficients are also given in Fig. 3. The accuracy of the approximation is within 1–1.5 dB, which is rather satisfactory, except for the low-density blocky particles.

Figure 4 shows ΔDR dependencies on particle aspect ratios for the quasi-linear slant-45° linear and quasi-circular polarizations achievable with the ETL K_a-band radar. One can see that the curves are compressed, and contrasts ΔDR for these polarizations are significantly lower in comparison with the perfect polarizations. These contrasts are somewhat better for the quasi-circular polarization (Figs. 4b and 4d) than for the quasi-linear slant-45° polarization (Figs. 4a and 4c). This is particularly noticeable for blocky particles with aspect ratios greater than about 0.7, for which the quasi-linear slant-45° polarization contrasts are less than 1 dB. The corresponding quasi-circular depolarization ΔDR contrasts exceed 1 dB ($r < 0.9$). This fact is of importance

for the problem of differentiating ice particles from spherical drizzle drops.

The coefficients of the cosine-type fits in Figs. 3 and 4 depend on particle bulk density and the polarization used. For the different polarization types considered here, density dependence of these coefficients was approximated by power-law functions

$$\Delta DR = a\cos(r^b\pi/2), \qquad a = x\rho^y, \qquad b = u\rho^w. \quad (14)$$

The coefficients x, y, u, and w are given in Table 1. The approximation (14) enables the estimation of particle aspect ratios for a given bulk density after the particle type (i.e., oblates vs prolates) is determined from the tendency of the elevation angle dependence of DR.

Modeling here was performed assuming that all particles in the radar sample volume have the same shapes and densities. In the case of a mixture of particles, estimations using (14) provide aspect ratios that represent reflectivity-weighted values, so the results will be indicative of the predominant particle types and shapes.

Propagation of radar signals through the media of nonspherical particles to and from the radar resolution volume increases the apparent depolarization ratio measured by radar compared to DR unaffected by propa-
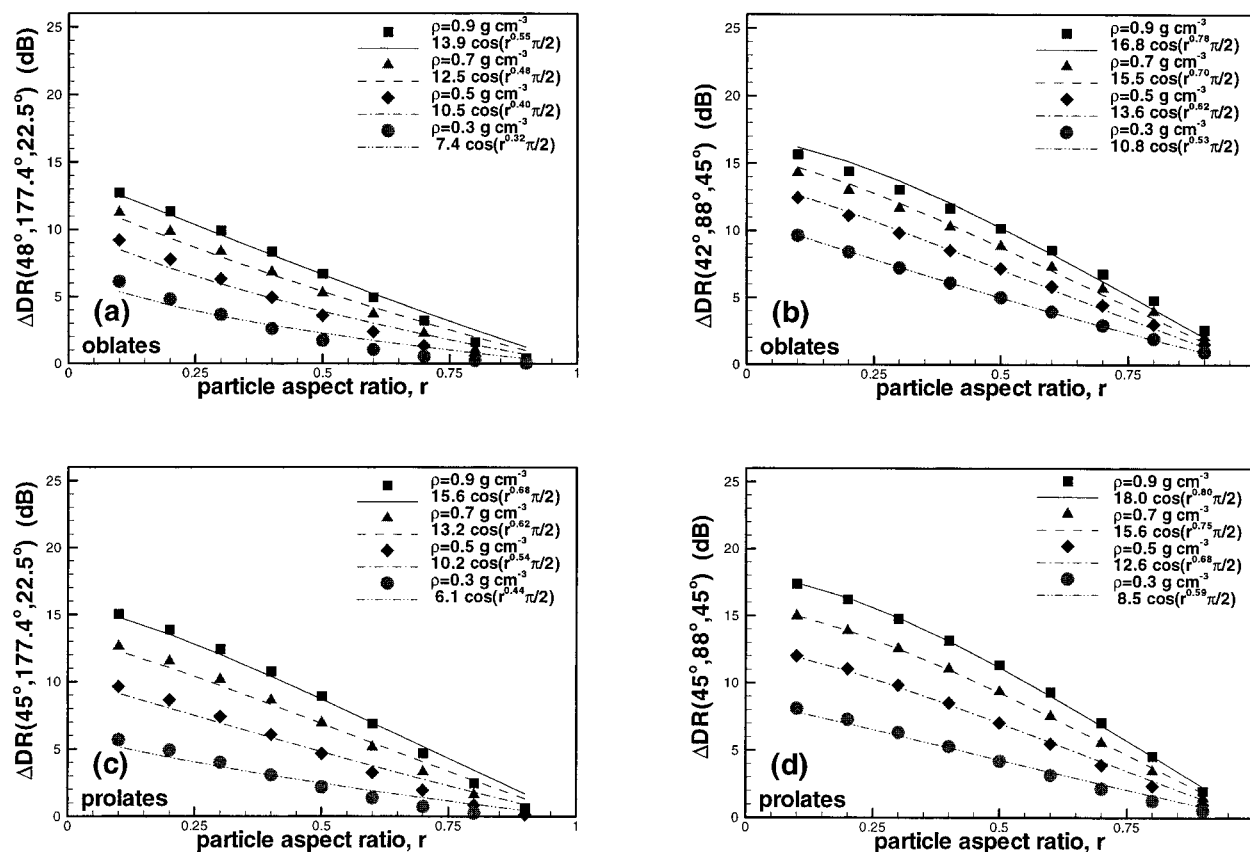
FIG. 4. Depolarization difference as a function of (a and b) oblate and (c and d) prolate particle aspect ratios for the elliptical polarizations with PRP phase shift angles 177.4° (a and c) and 88° (b and d).

gation. The propagation effects are more profound as elevation decreases, and they become stronger as particles along the propagation path become more non-spherical and particle bulk density increases. Unlike DR, which is a relative parameter, these effects depend on particle concentrations, so the apparent increase in DR becomes larger when cloud ice water content (IWC) increases.

The IWC values in winter clouds are not very large, however (usually not exceeding a few tenths of grams per meter cubed). Simple estimations show that for such IWC, the apparent increase of DR due to propagation does not exceed about 2 dB, even in the case of particles with very low aspect ratio ($r \approx 0.1$) viewed at elevations greater than about 30° at ranges under 10 km. Note also that since propagation effects tend to increase the ap-

parent DR monotonically, these effects, if significant, could be recognized by analyzing the DR range pattern.

It should be mentioned that propagation effects on DR are much smaller for the traditional linear polarization basis (i.e., H–V polarizations) than for the polarization bases considered here. This advantage of LDR measurements is, however, offset by the very low magnitude of radar signals backscattered onto the cross polarization by scatterers that are oriented mostly with their major dimensions in the horizontal plane, since the corresponding canting angles α for such orientations are small. This results in a high variability of LDR with α and also in very low LDR values at all elevation angles for oblates and at low elevation angles for prolates, which makes LDR impractical for the purpose of estimating particle shapes. As was mentioned above, how-

TABLE 1. Coefficients in the power-law approximations of ΔDR (dB) in Eq. (14).

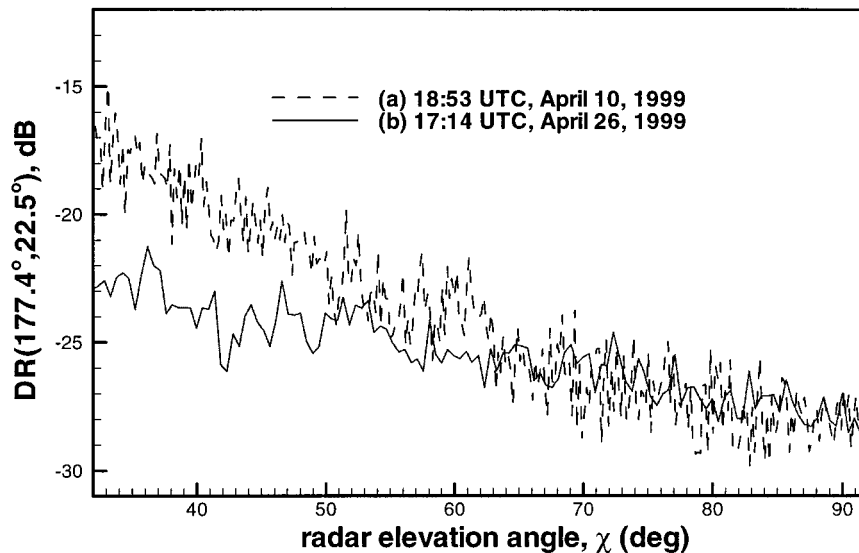| Polarization	Oblates				Prolates			
	x	y	u	w	x	y	u	w
$\Psi = 180°$, $\beta = 22.5°$	22.1	0.38	0.82	0.48	24.4	0.55	0.99	0.39
$\Psi = 90°$, $\beta = 45°$	27.7	0.32	0.97	0.45	26.8	0.49	1.09	0.37
$\Psi = 177.4°$, $\beta = 22.5°$	15.2	0.58	0.57	0.49	17.7	0.86	0.71	0.40
$\Psi = 88°$, $\beta = 45°$	17.8	0.41	0.80	0.35	19.7	0.69	0.83	0.28

FIG. 5. Elevation angle dependencies of DRs in (a) pristine and (b) rimed layers. Measurements are taken at 1.1 km altitude AGL.

ever, at very close ranges (e.g., aircraft based measurements) the ''weak'' signals in the H–V basis can, in principle, be strong enough to reconstruct returns at polarization bases where the influence of α is minimal.

4. Experimental examples

In April 1999, the ETL K_a-band radar was used in the Mount Washington Icing Sensors Program (MWISP), sponsored, in part, by the Federal Aviation Administration (FAA). The radar was deployed near the foot of Mount Washington in northern New Hampshire, approximately 4 km west of the summit. One of the ETL's objectives during this field experiment was to demonstrate the potential of the depolarization approach for identifying different particle types in winter clouds. The 177.4° PRP was used for this experiment in a slant mode, thus the measured DRs were DR(177.4°, 22.5°) according to the notation adopted above.

The main radar scanning mode included range–height indicator (RHI) scans along the azimuth direction to the summit (86.6°) of Mount Washington. The summit was located at a range of 3.8 km at 1.1 km above the radar site. A wealth of data in different types of winter clouds was collected during this month-long field experiment. Though the in-depth analysis of the MWISP results will be the subject of long-term subsequent research, some illustrations of the aforementioned theoretical findings are given below.

Figure 5a shows typical DR patterns from RHI scans through a layer of unaggregated pristine stellars (Fig. 5a) and heavily rimed dendrites (Fig. 5b). These crystal types were verified by in situ sampling. The scan rate for the pristine stellar RHI was about 4° s^{-1}, which resulted in a different data resolution than that for the

rimed dendrite RHI, where the scan rate was about 1.5° s^{-1}. The DRs are given for a fixed altitude of about 1100 m above the ground, which corresponds to the summit level. A strong monotonic decrease of DR with the increasing elevation angle is very pronounced for the pristine stellar case. This decrease is still very obvious, though not as prominent, for the case of rimed crystals, hence the oblate type of ice crystals can be still unmistakably determined.

It can be seen from Fig. 5 that ΔDR(48°, 177.4°, 22.5°) values are about 8.5 and 4 dB for the pristine and rimed cases, respectively. These values were determined from a polynomial fit to the experimental DR data, since the raw DR measurements are noisy. Pristine stellars sampled at the summit and near the base of the mountain had typical sizes of about 1–1.5 mm. Fig. 6a shows the image of a typical particle for this case as photographed by the Cloud Particle Imager (CPI) at the site of the Mount Washington Observatory. According to Heymsfield (1972), the bulk density of stellars is close to that of dendrites, and it is about 0.5 g cm^{-3} for 1.5-mm particles and increases with size, reaching about 0.6 g cm^{-3} for 0.9-mm particles. For the given polarization, this bulk density results in coefficients in (14) $a \approx 10.2$ and $b \approx 0.406$ (see Table 1). Applying (14) for estimations of oblate particle aspect ratios yields $r \approx 0.09$, which is close to typical aspect ratios of pristine stellars according to microphysical data given by Pruppacher and Klett (1978) and observed during this dendritic case. The 0.1 g cm^{-3} uncertainty in the assumed value of stellar bulk density (i.e., $\rho = 0.5 \pm 0.1$ g cm^{-3}) will cause variations in the estimated aspect ratios on the order of ± 0.07.

As a result of riming, the aspect ratio of crystals (r) diminishes, and this results in a smaller dynamic range
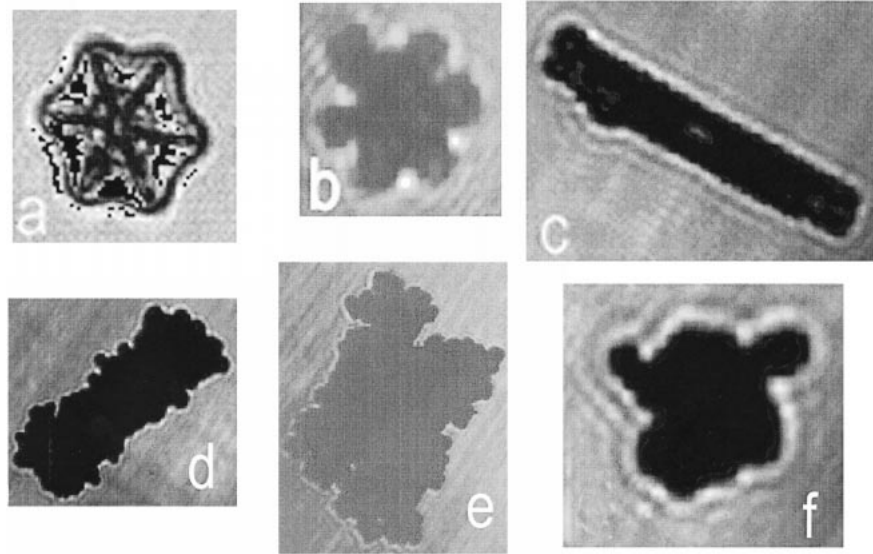
FIG. 6. Examples of cloud particle images taken during the (a) pristine stellar, (b) rimed dendrite, (c) long column, (d and e) rimed blocky column, and (f) graupel cases. Images are courtesy of the Stratton Park Engineering Company (SPEC), Inc.

of DR changes. Sometimes riming is an intermediate stage of a transition from pristine crystals to graupel. Estimating aspect ratios of rimed dendrites from experimental data using (14) for $\rho = 0.5 \pm 0.1$ g cm^{-3} yields $r \approx 0.45 \pm 0.09$, which is in good agreement with visual inspection of the particles. A CPI image of a typical rimed dendrite particle for this case is shown in Fig. 6b. Note that the greater bulk densities (i.e., $\rho \approx 0.6$ g cm^{-3}) could be more appropriate assumption for rimed dendrites, since riming sometimes results in increasing bulk densities (Heymsfield 1982).

Figure 7 (a and b) shows typical RHI patterns obtained in layers of columnar crystals. As expected, DRs for prolate-type particles exhibit practically no trend as a function of the radar elevation angle. Heymsfield (1972) points out that bulk densities of columnar crystals and bullets have a very weak dependence on size and usually vary from 0.65 to 0.85 g cm^{-3}. The data in Fig. 7 indicate that ΔDR(45°, 177.4°, 22.5°) for the 17 April and the 27 April columnar cases are about 11.8 and 5.3 dB, respectively. As in the planar cases, these values were found using a polynomial fit of the raw DR data. It can be seen from Fig. 4c and Eq. (14) that these values of ΔDR(45°, 177.4°, 22.5°) correspond to the aspect ratios $r \approx 0.2 \pm 0.1$ (for $\rho \approx 0.75 \pm 0.1$ g cm^{-3}) for the long column case of 17 April 1999. These es-
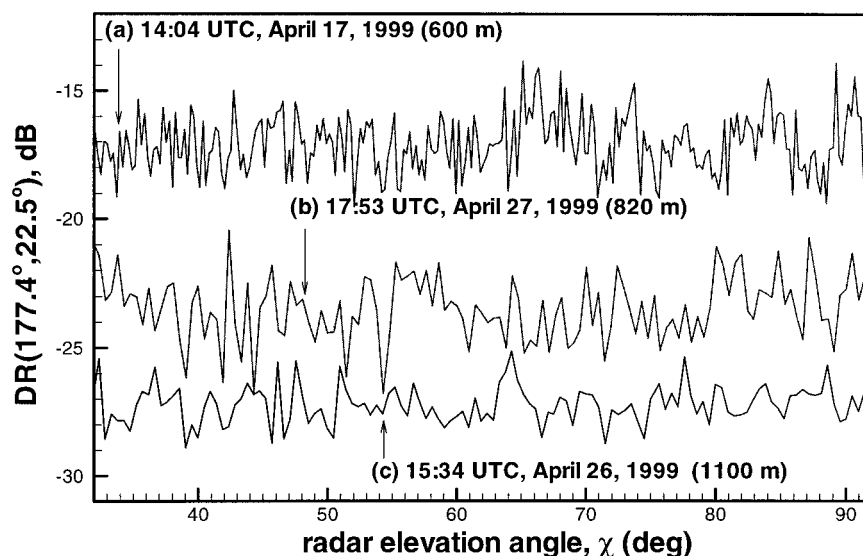

FIG. 7. Elevation-angle dependencies of DRs in (a and b) columnar layers and (c) in graupel layer.

timates correspond well to in situ observations near the radar site, which indicated falling columns with aspect ratios of about 0.2 and lengths of about 1.5 mm at approximately this time (i.e., 1400 UTC on 17 April). A corresponding CPI image taken at the Mount Washington Observatory during this case also reveals long columns with an aspect ratio of about 0.2 (see, e.g., crystal in Fig. 6c).

Theoretical estimates of columnar crystal aspect ratios for the case of 27 April 1999 yield $r \approx 0.6 \pm 0.1$ for the same interval of densities ($\rho \approx 0.75 \pm 0.1$ g cm^{-3}). According to in situ samples during this case, blocky columns with some riming were the predominant species. Figure 6d shows a CPI image of such a column taken at about the time of radar observations. Often these columns were bundled in pairs (see Fig. 6e). The resulting aspect ratios of particles during this case (Figs. 6d and 6e) are in general agreement with theoretical estimates from depolarization data.

Graupel particles usually have quasi-spherical, irregular, or conical shapes and can have a wide range of bulk densities from less than 0.2 to about 0.8 g cm^{-3} (Heymsfield 1982; Pruppacher and Klett 1978). Such shapes are difficult to characterize as either prolate or oblate. Given the low bulk densities and closeness of the aspect ratios to 1, it is expected that graupel DRs would be very low and close to the limiting case of spheres, which is -29 dB for the polarization state used in this experiment.

Figure 7c shows measurements of DR(177.4°, 22.5°) as a function of radar elevation angle for the graupel case observed during MWISP. Figure 6f shows an image of a typical particle taken by CPI during this case. It can be seen from Fig. 7c that the DR of graupel is very low and does not exhibit any significant trend with χ. At the same time, the mean value of DR(177.4°, 22.5°) is about -27.5 dB, which provides a detectable separation from the spherical case. This suggests the possibility for differentiating graupel from drizzle using depolarization measurements with this PRP.

The experimental examples discussed above provide a good illustration that the depolarization approach can be used for estimating aspect ratios of ice hydrometeors in winter clouds. These examples show that differentiation among mostly pristine planar crystals (such as stellars and dendrites), rimed dendrites, long columns, and blocky columns can be achieved using only DR data. The reliable quantitative estimations of particle aspect ratios, however, require knowledge of the particle bulk density. The density information in a potential remote sensing method can be assumed a priori based on reasonable or typical values, and the retrieval accuracies can be assessed based on the uncertainties of such an assumption. For a more elaborate development, the density information can be obtained, for example, from relations between bulk density and particle characteristic size when such size is inferred from auxiliary data such as dual-wavelength radar measurements. Such studies, however, are beyond the scope of the current research.

5. Conclusions

Depolarization ratio (DR) is one of the common observables that is measured by most polarization diversity radars. For a given incident polarization, this ratio is sensitive to scatterers' shape, orientation, and bulk density and thus can be used to infer information about hydrometeor species. In the traditional horizontal–vertical polarization basis, DRs exhibit strong dependence on scatterers' orientation masking effects of particle shape. The orientation effect is much weaker for circular and slant linear polarizations, which is an important advantage for identifying particles.

This article examined the potential for using circular, slant-45° linear, and two elliptical polarizations achievable with the NOAA K$_a$-band radar for the purpose of providing information on hydrometeor shapes. The two elliptical polarizations considered here are a quasi-circular polarization with the ellipticity of about 0.96 and a quasi-linear slant-45° polarization with the ellipticity of about 0.03. These polarizations are obtained with 88° and 177.4° phase retarding plates that are currently in use with this radar when the PRPs are rotated to 45° and 22.5°, respectively, with respect to horizontal. True circular and true linear slant-45° polarizations have not been achievable thus far.

Plate-type crystals (i.e., different types of plates, dendrites, and branched crystals, etc.) are readily distinguishable from the columnar-type crystals (i.e., columns, bullets, needles, etc.) by the variations of the DR with radar elevation angle χ. The DR monotonically decreases as this angle increases for plate-type crystals. Columnar-type crystals exhibit DR tendencies either to increase gradually with χ (e.g., for circular polarization) or to remain almost constant for a wide range of χ. For a given particle density ρ, DR increases as particle aspect ratio r decreases. Diminishing density results in a decrease of DR for a constant r.

For both particle types, there are certain radar elevation angles χ_o for which DR values do not depend much on the particle flutter around their otherwise mean horizontal orientation due to aerodynamic forcing. The DRs observed at these elevations angles DR(χ_o) depend only on particle aspect ratios and their bulk density. The difference (ΔDR) between DR(χ_o) and DRs for spherical particles is a convenient parameter to use for estimating particle aspect ratios given that the bulk density is known or assumed and particle type (i.e., plate-type vs columnar type) is established from the elevation angle trends. For the current ETL K$_a$-band radar, the corresponding DR values for spherical particles are -36 dB for the circular and linear polarizations and -29 dB for the two elliptical polarizations discussed here. Rigorous calculations of ΔDR as a function of particle aspect ratio and density for wide ranges of r and ρ were

performed. Empirical approximations of results of these calculations were derived for ΔDR as a function of particle aspect ratio and bulk density: ΔDR = f(r, ρ).

It was found that the quasi-circular polarization considered here provides larger contrasts ΔDR than the quasi-linear slant-45° polarization. This gives a stronger signal, which is then used to estimate particle aspect ratios from the derived approximations ΔDR = $f(r, \rho)$. This is especially important when trying to estimate aspect ratios for blocky particles and for any particles that have low bulk density. The use of elliptical polarizations results in a decrease of ΔDR in comparison with the perfect circular and slant-45° linear polarizations. The advantage of the elliptical polarizations, however, is in the increase of the received return power in the ''weak'' polarization channel, which makes it possible to observe depolarizations from lower reflectivity clouds than could be achieved with true circular and linear polarizations. This trade-off between the sensitivity and the dynamic range of the usable signal is a very important issue for the choice of the transmitted polarization.

Propagation effects tend to alter DRs, especially at lower elevations. Unlike DR values, these effects depend not only on particle shapes but also on their concentration and the range from the radar to the resolution volume. These effects could be recognized from a gradual increase of DR with range at lower elevations.

The suggested approach for estimating particle aspect ratios was illustrated using the data obtained during the April 1999 MWISP field experiment with the ETL K_a-band radar transmitting the quasi-linear slant-45° polarization. It was demonstrated that this approach allows rigorous identification of such particle species as mostly pristine planar crystals, rimed planar crystals, long columns, blocky columns, and graupel. Estimates of particle aspect ratios from depolarization measurements are in good agreement with estimates from in situ data when typical bulk densities for the observed species were assumed. The uncertainty in estimated aspect ratios is about 0.1 when the uncertainty of assumed bulk densities is ± 0.1 g cm^{-3}. More accurate information about particle bulk density from auxiliary measurements (e.g., dual-wavelength estimates of particle characteristic size and relating this size to bulk density) could lead to a better accuracy of aspect ratio estimations.

The approach discussed in this paper is intended mainly for layers with single shape hydrometeors. The experimental data collected in MWISP indicate that such layers commonly exist in winter clouds. In situations with a mixture of different hydrometeor species and for particles with different degrees of aggregation, the estimates of particle aspect ratios obtained using this approach would reflect characteristics of the predominant particle type.

REFERENCES

Aydin, K., and C. Tang, 1997: Millimeter wave radar scattering from model ice crystal distributions. *IEEE Trans. Geosci. Remote Sens.,* **35,** 140–146.

Bohren, C. F., and D. R. Huffman, 1983: *Absorption and Scattering of Light by Small Particles.* John Wiley and Sons, 530 pp.

Dungey, C. E., and C. F. Bohren, 1993: Backscattering by nonspherical hydrometeors as calculated by the coupled-dipole method: An application in radar meteorology. *J. Atmos. Oceanic Technol.,* **10,** 526–532.

Heymsfield, A. J., 1972: Ice crystal terminal velocities. *J. Atmos. Sci.,* **29,** 1348–1357.

——, 1982: A comparative study of the rates of development of potential graupel and hail embryos in High Plains storms. *J. Atmos. Sci.,* **39,** 2867–2897.

Holt, A. R., 1984: Some factors affecting the remote sensing of rain by polarization diversity radar in 3- to 35-GHz frequency range. *Radio Sci.,* **47,** 1399–1421.

Kropfli, R. A., and R. D. Kelly, 1996: Meteorological research applications of mm-wave radar. *Meteor. Atmos. Phys.,* **59,** 105–121.

Matrosov, S. Y., 1991: Theoretical study of radar polarization parameters obtained from cirrus clouds. *J. Atmos. Sci.,* **48,** 1062–1070.

——, and R. A. Kropfli, 1993: Cirrus cloud studies with elliptically polarized K_a-band radar signals. A suggested approach. *J. Atmos. Oceanic Technol.,* **10,** 684–692.

——, R. F. Reinking, R. A. Kropfli, and B. W. Bartram, 1996: Estimation of ice hydrometeor types and shapes from radar polarization measurements. *J. Atmos. Oceanic Technol.,* **13,** 85–96.

Oguchi, T., 1983: Electromagnetic wave propagation and scattering in rain and other hydrometeors. *Proc. IEEE,* **71,** 1029–1078.

Pruppacher, H. R., and J. D. Klett, 1978: *Microphysics of Clouds and Precipitation.* D. Reidel, 714 pp.

Reinking, R. F., S. Y. Matrosov, R. T. Bruintjes, and B. E. Martner, 1997a: Identification of hydrometeors with elliptical and linear polarization K_a-band radar. *J. Appl. Meteor.,* **36,** 323–339.

——, ——, B. E. Martner, and R. A. Kropfli, 1997b: Differentiation of freezing drizzle from ice hydrometeors and freezing rain with dual-polarization radar. *J. Aircraft,* **34,** 778–784.

Sassen, K., 1980: Remote sensing of planar ice crystal fall attitudes. *J. Meteor. Soc. Japan,* **58,** 422–429.

Shurcliff, W. A., 1962: *Polarized Light.* Harvard University Press, 208 pp.

Torlashi, E., and A. R. Holt, 1999: A comparison of different polarization schemes for the radar sensing of precipitation. *Radio Sci.,* **33,** 1335–1352.

Vivekanandan, J., D. S. Zrnić, S. M. Ellis, R. Oye, A. V. Ryzhkov, and J. Straka, 1999: Cloud microphysical retrieval using S-band dual-polarization radar measurements. *Bull. Amer. Meteor. Soc.,* **80,** 381–388.

Zrnić, D. S., and A. V. Ryzhkov, 1999: Polarimetry for weather surveillance radars. *Bull. Amer. Meteor. Soc.,* **80,** 389–406.